Drug Delivery

International Edition: DOI: 10.1002/anie.201505913
German Edition: DOI: 10.1002/ange.201505913

Detecting Cytosolic Peptide Delivery with the GFP Complementation Assay in the Low Micromolar Range

*Samuel Schmidt, Merel J. W. Adjobo-Hermans, Rike Wallbrecher, Wouter P. R. Verdurmen, Petra H. M. Bovée-Geurts, Jenny van Oostrum, Francesca Milletti, Thilo Enderle, and Roland Brock**

Abstract: *Transfection of cells with a plasmid encoding for the first ten strands of the GFP protein (GFP1-10) provides the means to detect cytosolic peptide import at low micromolar concentrations. Cytosolic import of the eleventh strand of the GFP protein either by electroporation or by cell-penetrating peptide-mediated import leads to formation of the full-length GFP protein and fluorescence. An increase in sensitivity is achieved through structural modifications of the peptide and the expression of GFP1-10 as a fusion protein with mCherry.*

There is great interest in exploiting peptides and peptide-derived molecules as drugs to address the intracellular target space. Cell-penetrating peptides (CPPs) and related molecules are receiving considerable attention as delivery vectors.[1] However, efficient cytoplasmic delivery is still a major hurdle as uptake occurs mostly through endocytosis, and no generic concept has been developed to achieve either direct penetration of the plasma membrane or endosomal release.[2] A key prerequisite in the further development of delivery vectors is the availability of a robust technique to assess cytosolic delivery of the intact molecule. For molecules small enough to pass the nuclear pore complex, which is of a molecular weight of below around 40 kDa, this is also equivalent to nuclear delivery. For the delivery of oligonucleotides, it has been shown that import efficiency as measured by cell-associated fluorescence of various labeled CPP-oligonucleotide complexes does not correlate well with biological activity.[3] Therefore, cytosolic delivery of intact oligonucleotides is determined by functional assays, such as the splice-correction assay.[4] For delivery strategies geared towards enzymes and large molecular weight proteins, import efficiency can be measured by detecting enzymatic activity.[5] Luciferin has been employed as a model compound to detect the delivery of small molecules, and dexamethasone-induced gene expression as a general means to detect endosomal release. Both methods, though, do not provide information about the integrity of the carrier to which the drug is attached.[6]

By contrast, the quantitation of CPP-mediated peptide delivery has mainly relied on the detection of peptide-coupled fluorescence. However, as shown by our own fluorescence correlation spectroscopy (FCS) and Förster energy resonance transfer-based analyses, most cytosolic fluorescence originates from fluorophores coupled to degraded peptide fragments.[7] Therefore, the implementation of functional assays that quantitate the cytosolic delivery of intact peptides is urgently needed. Mass spectrometry-based analyses address some of these problems.[8] But also with this approach, it remains a challenge to distinguish cytosolic delivery from sequestration into endosomes. Furthermore, it is difficult to foresee how this approach could be implemented in preclinical in vivo studies.

Ideally, a functional assay should enable a robust read-out based on signal intensity and should directly probe for the molecular interaction of a functional peptide, as this corresponds to a potential application of peptides as therapeutics. Examples of functional assays include induction or enhancement of apoptosis. However, these are difficult to relate to a certain concentration of active peptide interacting with a specific target protein.[9]

Herein, we demonstrate that complementation of a GFP fragment consisting of the first 10 of the 11 strands of the GFP β-barrel (GFP1-10) with a second fragment, the 16 amino acid long 11th strand can be used to detect cytosolic peptide delivery. The spontaneous association of both fragments is required for the generation of GFP fluorescence.[10] GFP1-10 complementation is detectable at submicromolar concentrations of GFP11 when GFP1-10 is present at low micromolar concentrations.[10,11] This strand complementation assay is one of the so-called fragment complementation assays, and to our knowledge the only one in which one part comprises a fragment of the size of a peptide.[12] We demonstrate that the sensitivity and robustness of the assay can be further increased by generating a fusion protein of GFP1-10 with the red fluorescent mCherry protein, and through structural

[*] S. Schmidt, Dr. M. J. W. Adjobo-Hermans, Dr. R. Wallbrecher, Dr. W. P. R. Verdurmen,[+] P. H. M. Bovée-Geurts, J. van Oostrum, Prof. Dr. R. Brock
Department of Biochemistry (286)
Radboud Institute for Molecular Life Sciences
Radboud University Medical Center
Geert Grooteplein 28, 6525 GA Nijmegen (The Netherlands)
E-mail: roland.brock@radboudumc.nl

Dr. F. Milletti
Roche Pharmaceutical Research and Early Development
Roche Innovation Center New York
430 East 29th Street, 10016 New York, NY (USA)

Dr. T. Enderle
Roche Pharmaceutical Research and Early Development
Roche Innovation Center Basel, F. Hoffmann-La Roche Ltd
Grenzacherstrasse 124, 4070 Basel (Switzerland)

[+] Present address: Department of Biochemistry
University of Zurich
Winterthurerstrasse 190, 8057 Zurich (Switzerland)

Supporting information for this article is available on the WWW under http://dx.doi.org/10.1002/anie.201505913.

modifications of the GFP11 peptide. Moreover, we identify incubation time as a critical parameter. Overall, we are able to detect complementation at low micromolar peptide concentrations.

To test whether elongation of the GFP11 peptide with a CPP interfered with complementation, HEK293T cells were transfected with GFP1-10 while GFP11 peptides were introduced directly into the cytoplasm by electroporation. Next to GFP11, we tested GFP11 elongated with R9 and an R9-GFP11 analogue elongated with the C-terminal PEG-moiety Ado (8-amino-3,6-dioxaoctanoic acid) and in which the methionine was replaced by a sterically very similar norleucine (Nle) (Supporting Information, Figure S5 A, B). The C-terminal Ado elongation is expected to increase proteolytic stability and solubility of the peptide, while replacement of the methionine residue should circumvent problems associated with the oxidation of methionine.

Following electroporation, cells could recover for 20 min and 2 h. The 2 h recovery was selected in accordance with the previously reported kinetics for GFP complementation.[13] The 20 min recovery time was selected because inside cells proteolysis can lead to a rapid depletion of complementation-active molecules.

For the 2 h recovery, there was a dose-dependent increase in GFP fluorescence for all three peptides (Figure 1 A), which was the result of a uniform shift of the whole cell population (Supporting Information, Figure S1 A). Our previous work had shown that using electroporation, the concentration of peptide inside the cell is always lower than the concentration outside.[14] Therefore, the concentrations in the electroporation solution are an upper limit for the concentration expected in the cytosol.

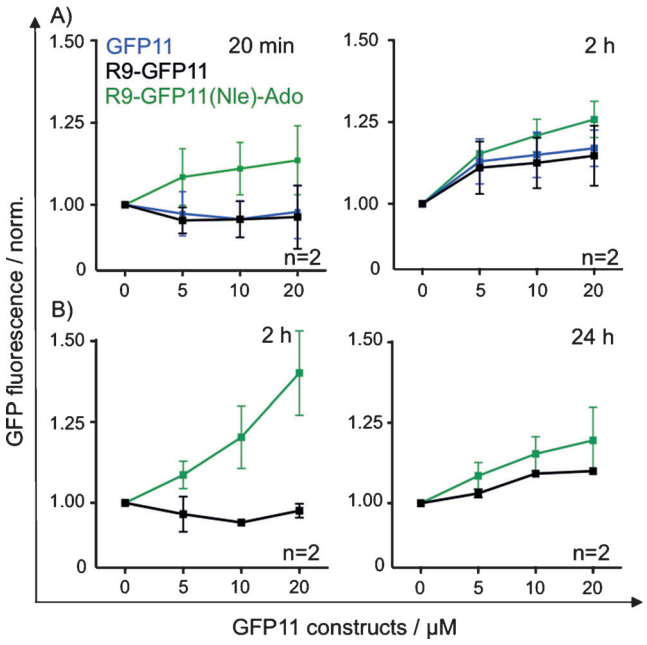

Figure 1. Dose-dependence of GFP complementation. GFP11 peptides were introduced into HEK293T cells transfected with standard GFP1-10 either by A) electroporation or by B) penetration. Fluorescence of GFP was detected by flow cytometry from morphologically intact cells gated based on forward versus sideward scatter at the indicated time points. The GFP fluorescence of the GFP11 variants was normalized to the background signal acquired from mock-treated cells. Curves indicate the average of the normalized medians of two independent experiments. Error bars = standard error of the mean (SEM).

There was no difference in complementation efficiency for GFP11 and the R9-elongated peptide (Figure 1 A), demonstrating that elongation with the CPP was compatible with complementation. The (Nle)-Ado modified peptide was slightly more efficient than the non-modified peptide.

In contrast, for the short 20 min recovery time, only for the modified peptide, an increase in fluorescence could be observed while there was no activity for the unmodified peptides (Figure 1 A; Supporting Information, Figure S2 A). This difference in activity was not a result of a difference in import efficiency as carboxyfluorescein-labeled analogues of all the peptides showed only slight differences in the dose-dependent electroporation efficiencies (Supporting Information, Figure S3).

After electroporation, we assessed complementation for detecting the CPP-mediated import of peptides. Again, the modified peptide (R9-GFP11(Nle)-Ado) was more active than the unmodified one (R9-GFP11), and this difference was more pronounced for the 2 h than for the 24 h penetration. Importantly, a reproducible increase in fluorescence at 5 μM could be observed, with a stronger intensity after the 2 h compared to the 24 h incubation (Figure 1; Supporting Information, Figures S1 B and S2 B). As for introduction by electroporation, the enhanced signal increase by the modified peptide could not be explained by differences in uptake efficiency or subcellular distribution. Carboxyfluorescein-labeled analogues of R9-GFP11 and R9-GFP11(Nle)-Ado showed equal levels of CPP-mediated uptake over the tested concentration range of 2.5 to 20 μM (Supporting Information, Figure S4). For both peptides, in addition to some punctate staining, fluorescence was distributed homogeneously throughout the cytoplasm and nucleus over the whole concentration range, indicating that the peptides were available for complementation.

Even though we found a high number of fluorescent cells, the implementation of the assay as such still provided insufficient information on the efficiency of delivery. In particular, in transient expression procedures, expression levels between cells are variable and many cells may not express the transfected protein at all. Low fluorescence can therefore be a consequence of poor peptide delivery or of poor expression of GFP1-10. Therefore, to obtain reliable information on GFP1-10 expression, we created a fusion protein with mCherry at the N-terminus of GFP1-10 (Supporting Information, Figure S5). We reasoned that in this configuration, the mCherry would also stabilize the GFP1-10.

Consistent with a stabilizing role of mCherry, electroporation of peptides into cells expressing the fusion protein yielded stronger increases in fluorescence than for GFP1-10, and this was particularly the case for the 20 min recovery time with a maximum increase of 1.75 versus 1.15 seen for the (Nle)-Ado modified peptide (Figures 1 A and 2 A). Gating on mCherry-positive cells (Supporting Information, Figure S6) increased the average fluorescence, resulting in a detection of complementation at 5 μM for all peptides (Figure 2).

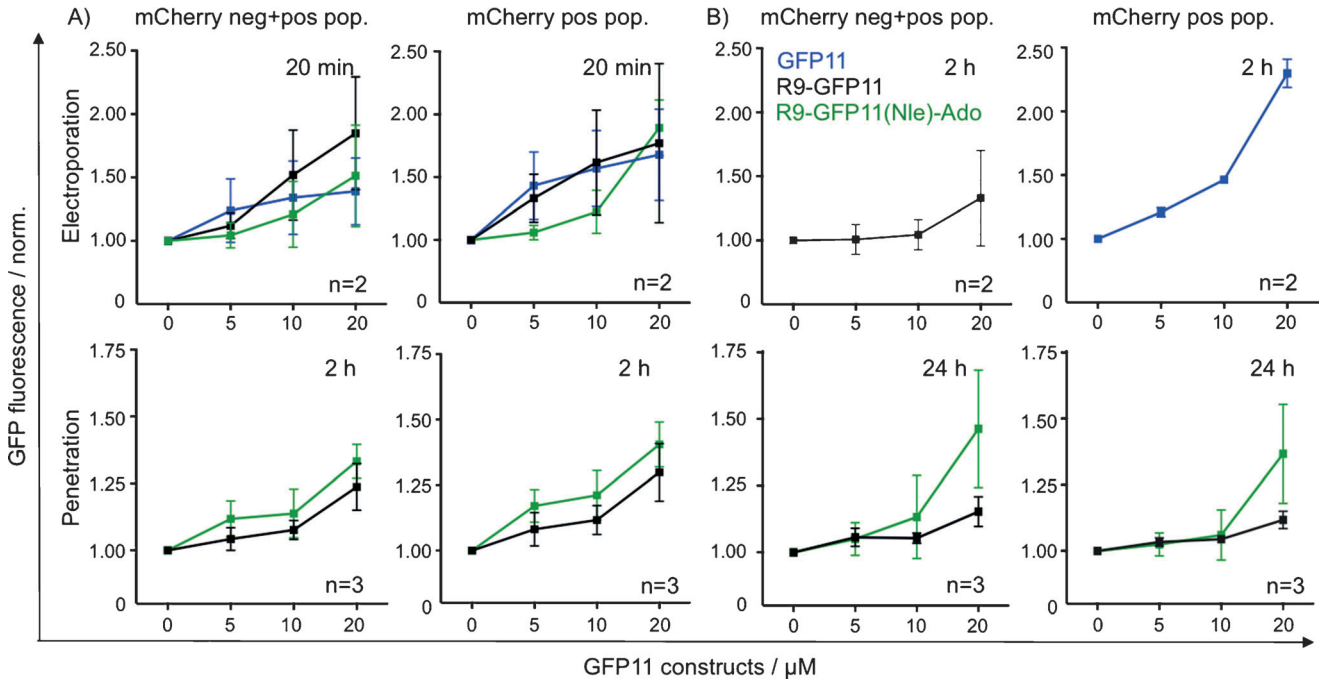

Figure 2. Dose-dependence of GFP complementation for the mCherry-GFP1-10 fusion protein after short (A) or long term (B) incubation. GFP11 peptides were introduced into HEK293T cells transfected with mCherry-GFP1-10. Fluorescence for both mCherry and GFP was detected by flow cytometry from morphologically intact cells gated based on forward versus sideward scatter after A) 20 min or B) 2 h (electroporation, top) or A) 2 h or B) 24 h (penetration, bottom). Incubation for 24 h was performed in FCS-containing medium. The GFP fluorescence of the GFP11 variants either for all cells (left) or for mCherry-positive cells was normalized to the background signal acquired from mock-treated cells. Curves indicate the average of the normalized medians of at least two independent experiments. Error bars = standard error of the mean (SEM).

At this point we were also interested in defining in more detail the dose-response function of GFP complementation. For this purpose, pairs of samples were electroporated either with the fluorescein-labeled peptide and cell-associated fluorescence determined by flow cytometry, or with the non-fluorescent counterpart to determine GFP formation. For the fluorescein-labeled peptide, there was a nearly linear increase in cellular fluorescence with peptide concentration. In contrast, for GFP complementation, from 10 to 20 μM of peptide the increase in fluorescence was weaker than expected, indicating saturation effects of the complementation reaction (Supporting Information, Figure S7).

For CPP-mediated import, again, the increase in fluorescence was stronger for the (Nle)-Ado analogue than for the unmodified peptide (Figure 2; Supporting Information, Figure S6).

A further analysis of the subpopulations of mCherry-positive and -negative cells also revealed that the population of cells with little mCherry expression showed a dose-dependent increase in GFP signal (Supporting Information, Figures S6 and S8). The molecular basis for this observation is not clear. Since differences in reporter protein expression may reflect a stronger propensity of cells to take up material, we validated that uptake of R9-GFP11 was independent of mCherry-GFP1-10 expression (Supporting Information, Figure S9). Furthermore, treatment of mCherry-GFP1-10 expressing cells with R9 alone, or of mock-transfected cells with R9-GFP11, did not show any signal (Supporting Information, Figure S10), validating that the observed increase in GFP fluorescence was a consequence of complementation (Figure 2).

For both GFP1-10 constructs, complementation was more efficient after 2 h incubation than after 24 h incubation (Figures 1 B and 2; Supporting Information, Figures S6 B and S8 B). In addition to the degradation of peptide and protein turnover, another factor contributing to this difference might be the presence of serum in the incubation medium, which reduces the bioavailability of peptide.[15] The 2 h incubations were conducted in the absence of serum, while the 24 h incubation was performed in the presence of serum to maintain cell viability.

After having identified a 2 h incubation period as the optimal condition for detecting complementation, we were interested to learn whether complementation could also be detected at lower concentrations of peptide. In fact, GFP fluorescence could already be detected at 0.6 μM, which was slightly more pronounced for the (Nle)-Ado modified peptide than for the unmodified R9-GFP11. However, between 0.6 and 2.5 μM there was no clear dose-dependent increase of fluorescence. Incubation of cells with the R9-GFP11 peptides at very high concentrations (40 μM) resulted in a further increase of GFP fluorescence, demonstrating that the assay can also be used at even higher concentrations, even though at these concentrations CPP-mediated toxicity may become a concern (Supporting Information, Figure S11).

To demonstrate that cytosolic delivery is the decisive factor for detection of complementation, we manipulated the composition of the plasma membrane by treatment of HeLa cells with bacterial sphingomyelinase. Bacterial sphingomyelinase converts sphingomyelin into ceramide, which in turn leads to the rapid cytosolic delivery of arginine-rich CPPs and

conjugates.[16] We selected HeLa cells because they showed a stronger endosomal confinement of fluorescence than HEK293T cells. For the unmodified peptide, complementation efficiency was clearly increased for the sphingomyelinase-treated cells (Figure 3).

To conclude, we presented a complementation assay to detect CPP-mediated delivery of intact peptides into the cytoplasm, based on the formation of a fluorescent GFP by integration of a peptide corresponding to the eleventh

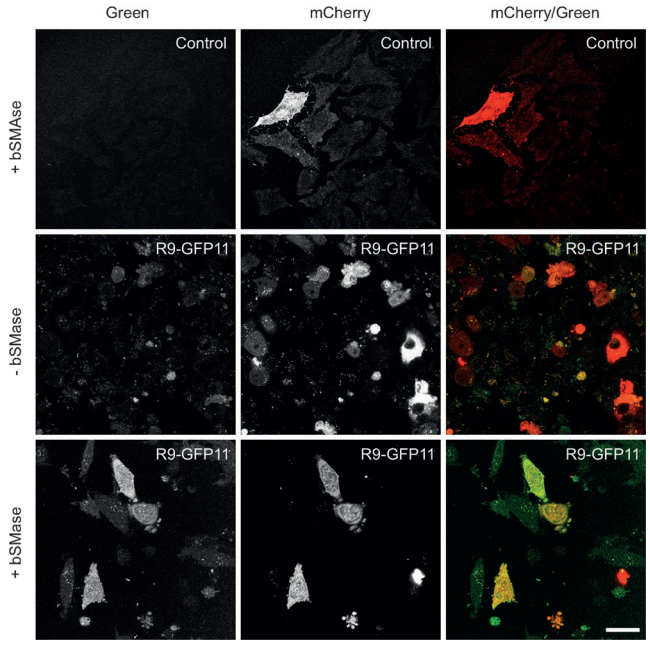

Figure 3. Change in membrane structure through induction of ceramide formation induces an increase in GFP complementation. HeLa cells were transfected with mCherry-GFP1-10 and incubated with 5 μM R9-GFP11 in the presence or absence of bSMase (1200 mU mL^{-1}) for 20 min at 37 °C followed by confocal microscopy. As a background control, transfected cells were incubated only in the presence of bSMAse (1.200 mU mL^{-1}). Green fluorescence indicates the presence of complemented GFP. Scale bar = 30 μm.

β-strand. Improvements in sensitivity were achieved by modifying the original GFP11 sequence and by expressing a two-domain construct in which GFP1-10 is linked to the C-terminus of mCherry. As a first application, we demonstrate that sphingomyelinase treatment of cells increases the permeability of the plasma membrane for direct cytoplasmic delivery of the peptide. We foresee future applications in testing strategies to enhance endosomal release, or characterization of carriers with respect to their capacity to mediate direct crossing of the plasma membrane. With the generation of stable cell lines, the assay should be readily compatible with high-throughput formats. Even though the assay does not report on the integrity of the carrier, research in delivery typically aims at the integrity of the cargo, and this is captured by the GFP complementation. The extent of complementation obtained by electroporation was not qualitatively different from the one obtained by penetration and also the sensitivity was comparable. A concentration of 5 μM in the electroporation cuvette yields a low micromolar peptide concentration inside the cytosol.[14] This result demonstrates that CPP-mediated import for HEK cells yielded similar cytoplasmic concentrations. The sensitivity of this assay is rather controlled by the affinity of the GFP1-10 fragment for the peptide than by lack of cytosolic delivery.

Acknowledgements

This work was supported by the Roche postdoctoral program.

Keywords: cell uptake · cell-penetrating peptides · drug delivery · fragment complementation assays · lipid membranes

[1] a) D. M. Copolovici, K. Langel, E. Eriste, U. Langel, *ACS Nano* **2014**, *8*, 1972 – 1994; b) P. Lonn, S. F. Dowdy, *Expert Opin. Drug Delivery* **2015**, 1 – 10.
[2] a) K. Cleal, L. He, P. D. Watson, A. T. Jones, *Curr. Pharm. Des.* **2013**, *19*, 2878 – 2894; b) R. Brock, *Bioconjugate Chem.* **2014**, *25*, 863 – 868.
[3] F. Said Hassane, R. Abes, S. El Andaloussi, T. Lehto, R. Sillard, U. Langel, B. Lebleu, *J. Controlled Release* **2011**, *153*, 163 – 172.
[4] S. El Andaloussi, P. Guterstam, U. Langel, *Nat. Protoc.* **2007**, *2*, 2043 – 2047.
[5] J. S. Wadia, R. V. Stan, S. F. Dowdy, *Nat. Med.* **2004**, *10*, 310 – 315.
[6] a) E. Eiríksdóttir, I. Mäger, T. Lehto, S. El Andaloussi, U. Langel, *Bioconjugate Chem.* **2010**, *21*, 1662 – 1672; b) J. M. Holub, J. R. Larochelle, J. S. Appelbaum, A. Schepartz, *Biochemistry* **2013**, *52*, 9036 – 9046.
[7] a) I. R. Ruttekolk, W. P. Verdurmen, Y. D. Chung, R. Brock, *Methods Mol. Biol.* **2011**, *683*, 69 – 80; b) R. Fischer, D. Bachle, M. Fotin-Mleczek, G. Jung, H. Kalbacher, R. Brock, *ChemBioChem* **2006**, *7*, 1428 – 1434.
[8] F. Burlina, S. Sagan, G. Bolbach, G. Chassaing, *Angew. Chem. Int. Ed.* **2005**, *44*, 4244 – 4247; *Angew. Chem.* **2005**, *117*, 4316 – 4319.
[9] a) M. Fotin-Mleczek, S. Welte, O. Mader, F. Duchardt, R. Fischer, H. Hufnagel, P. Scheurich, R. Brock, *J. Cell Sci.* **2005**, *118*, 3339 – 3351; b) I. R. Ruttekolk, A. Chakrabarti, M. Richter, F. Duchardt, H. Glauner, W. P. Verdurmen, J. Rademann, R. Brock, *Mol. Pharmacol.* **2011**, *79*, 692 – 700.
[10] S. Cabantous, T. C. Terwilliger, G. S. Waldo, *Nat. Biotechnol.* **2005**, *23*, 102 – 107.
[11] F. Pinaud, M. Dahan, *Proc. Natl. Acad. Sci. USA* **2011**, *108*, E201 – 210.
[12] S. W. Michnick, P. H. Ear, E. N. Manderson, I. Remy, E. Stefan, *Nat. Rev. Drug Discovery* **2007**, *6*, 569 – 582.
[13] L. Kaddoum, E. Magdeleine, G. S. Waldo, E. Joly, S. Cabantous, *Biotechniques* **2010**, *49*, 727 – 736.
[14] I. R. Ruttekolk, J. J. Witsenburg, H. Glauner, P. H. Bovee-Geurts, E. S. Ferro, W. P. Verdurmen, R. Brock, *Mol. Pharm.* **2012**, *9*, 1077 – 1086.
[15] M. Kosuge, T. Takeuchi, I. Nakase, A. T. Jones, S. Futaki, *Bioconjugate Chem.* **2008**, *19*, 656 – 664.
[16] W. P. Verdurmen, M. Thanos, I. R. Ruttekolk, E. Gulbins, R. Brock, *J. Controlled Release* **2010**, *147*, 171 – 179.

Received: June 27, 2015
Revised: October 5, 2015
Published online: ■■ ■■, ■■■■

Communications

Drug Delivery

S. Schmidt, M. J. W. Adjobo-Hermans, R. Wallbrecher, W. P. R. Verdurmen, P. H. M. Bovée-Geurts, J. van Oostrum, F. Milletti, T. Enderle, R. Brock* ——— ▮▮▮▮–▮▮▮▮

Detecting Cytosolic Peptide Delivery with the GFP Complementation Assay in the Low Micromolar Range

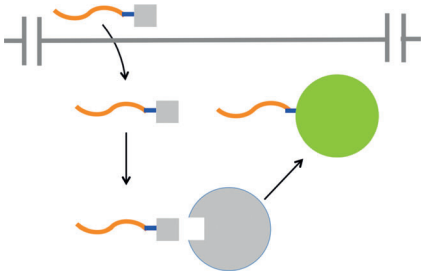

Peptide-based GFP complementation: Cells expressing the GFP1-10 GFP fragment (gray circle) are electroporated or penetrated with GFP-11 (gray squares), conjugated by a linker (blue line) to a CPP (orange line), resulting in the delivery into the cytosol and GFP complementation and fluorescence (green circle).

Angewandte Chemie
Eine Zeitschrift der Gesellschaft Deutscher Chemiker

Supporting Information

Detecting Cytosolic Peptide Delivery with the GFP Complementation Assay in the Low Micromolar Range

*Samuel Schmidt, Merel J. W. Adjobo-Hermans, Rike Wallbrecher, Wouter P. R. Verdurmen, Petra H. M. Bovée-Geurts, Jenny van Oostrum, Francesca Milletti, Thilo Enderle, and Roland Brock**

anie_201505913_sm_miscellaneous_information.pdf

Supporting Information

Table of contents

	Page
Materials and Methods	2-5
Supplemental Figure 1: Dose dependence of GFP complementation after long-term recovery and penetration.	6
Supplemental Figure 2: Dose dependence of GFP complementation after short-term recovery and penetration.	7
Supplemental Figure 3: Comparison of electroporation efficiencies.	8
Supplemental Figure 4: Concentration dependence of import and intracellular peptide distribution for Carboxyfluorescein-labeled analogs.	9
Supplemental Figure 5: The peptide sequence of Carboxyfluorescein-labeled and acetylated R9-GFP11 variants and the amino acid sequence of the mCherry-GFP1-10 fusion protein.	10
Supplemental Figure 6: Density plots showing the dose dependence of GFP complementation after short-term treatment with GFP11 variants.	11
Supplemental Figure 7. The dose dependent GFP fluorescence intensity is based on the cytosolic concentration of the GFP-11 variants.	12
Supplemental Figure 8: Density plots showing the dose dependence of GFP complementation after long-term treatment with GFP11 variants.	13
Supplemental Figure 9. Density plots showing equivalent uptake efficiencies of carboxyfluorescein labeled R9-GFP11 analogs in high and low mCherry-GFP1-10 expressing cells	14
Supplemental Figure 10: Density plots for control samples.	15
Supplemental Figure 11. Dose dependence of GFP complementation for the mCherry-GFP1-10 fusion protein after short-term incubation with GFP11 peptides at low concentrations.	16

Cell culture. HeLa and HEK293T cells (DSMZ) were maintained in RPMI 1640 and DMEM (Gibco, Invitrogen, Eugene, U.S.A.), respectively, supplemented with 10 % fetal calf serum (FCS; PAN Biotech, Aidenbach, Germany). All cells were incubated at 37°C in a 5 % CO_2-containing, humidified incubator. Cells were passaged every 2 to 3 days. For cell detachment phosphate-buffered saline (PBS) containing 2 mM EDTA was used.

Constructs and peptides. The DNA encoding GFP1-10 and mCherry-GFP1-10 (Supplemental Fig. 5) was synthesized and cloned into the pUC57 plasmid at Baseclear (Leiden, The Netherlands). The synthesized DNA was produced such that it was flanked by an EcoRI-site upstream and a BamHI-site downstream of the coding region. GFP1-10 / mCherry-GFP1-10 were excised from pUC57 with EcoRI and BamHI and ligated into the mammalian expression vector pcDNA3.1+ (Invitrogen, Eugene, U.S.A.). All constructs were verified by sequencing. Peptides were purchased as C-terminal peptide amides from EMC microcollections (Tübingen, Germany). The N-terminus was either capped by acetylation or by a Carboxyfluorescein moiety.

Transfection with GFP1-10. For peptide delivery by electroporation HEK293T cells were seeded in 6-well plates with 250,000 cells, for incubation and flow cytometry in 48-well plates with 40,000 cells and for confocal microscopy in 8-well microscopy chambers (IBIDI, München, Germany) with 40,000 cells per well in DMEM with FCS (10%) and cultured overnight at 37°C, 5% CO_2. HeLa cells were seeded in 8-well microscopy chambers (IBIDI, München, Germany) with 40,000 cells per well in RPMI 1640 with FCS (10%) and cultured overnight at 37°C, 5% CO_2. The next day,

the culture medium was replaced and cells were transfected with GFP1-10 / mCherry-GFP1-10 plasmid via lipofectamine 2000 (Invitrogen, Eugene, U.S.A.) under adherent condition. After 24 h (HEK293T) or 7 h (HeLa) incubation, the medium was replaced by fresh culture medium containing 10% FCS and the cells were cultured overnight.

Flow cytometry. For detection of GFP complementation flow cytometry was performed on a CyAn ADP flow cytometer (Beckman Coulter, Woerden, The Netherlands) using spectral ranges 530/40 for GFP and 613/20 for mCherry. Flow cytometry data of cells, electroporated with Carboxyfluorescein-labeled GFP11 variants were aquired using a BD FACS-Calibur (BD Biosciences, Erembodegem, Belgium) flow cytometer with a 488 nm argon ion laser. FCS Express Version 5 Research Edition (De Novo Software, Los Angeles, CA) was used for the analysis of the generated data. Per sample, 10,000 morphologically intact cells were gated based on forward versus sideward scatter and analyzed.

Electroporation of GFP11 variants. HEK293T cells were harvested using PBS containing 2 mM EDTA followed by 3 washing steps with PBS. 100 µl Ingenio Electroporation solution (Mirus Bio LLC, Madison, U.S.A.), containing the indicated peptides at the specified concentrations, was added with a final cell density of $5x10^5$ cells / 100 µl. The solution was transferred to a Mirus Bio Ingenio 0.2 cm cap electroporation cuvette (Sopachem, Ochten, The Netherlands). Cells were electroporated with an Amaxa Nucleofector II device using program A-023. 500 µl pre-warmed cell culture medium with 10% FCS was administered and cells were removed from the cuvette, transferred to a 10 ml tube, filled with pre-warmed serum-

containing culture medium and returned to the incubator either for 20 min or for 2 h to recover from the transfection procedure. Afterwards, cells were centrifuged, the pellet was resuspended in serum-containing medium without phenol red, transferred into tubes and flow cytometry was performed.

CPP-mediated import of GFP11 variants. The medium of adherent HEK293T cells was replaced by 150 µL DMEM. For incubation over 24 h, the medium was supplement with 10% FCS. Either R9-GFP11 or R9-GFP11(NLe)-Ado was administered at the indicated concentrations by adding a 150 µL premix followed by an incubation for either 2 h or 24 h. Afterwards cells were detached using PBS containing 2 mM EDTA, transferred into tubes and flow cytometry was performed.

Confocal microscopy. For microscopy of Carboxyfluorescein-labeled GFP11 analogs, HEK293T cells were seeded in 8-well microscopy chambers with 40,000 cells per well in DMEM with FCS (10%) and cultured overnight at 37°C, 5% CO_2. The next day, medium of the cells was replaced by 150 µl DMEM without phenol red and FCS. Cell culture medium containing the indicated concentrations of Fluo-R9-GFP11 or Fluo-R9-GFP11 (Nle)-Ado) was prepared as pre-mix and transferred to the IBIDI 8 well microscopy chambers. Confocal images were acquired 20 minutes after peptide administration. Confocal microscopy was performed on a TCS SP5 confocal microscope (Leica Microsystems, Mannheim, Germany) equipped with an HCX PL APO 63x 1.2 N.A. water immersion lens. Carboxyfluorescein fluorescence was excited using the 488 nm line of an argon ion laser and fluorescence detected at 500 - 550 nm. To assess the impact of sphingomyelinase treatment on complementation the medium of HeLa cells in 8-well microscopy chambers was replaced by 150 µl RPMI

1640 without phenol red and FCS. DMEM containing 2.5, 5.0, 10.0 or 20.0 μM R9-GFP11 or R9-GFP11 and 1.200 mU/ml bacterial sphingomyelinase (bSMase) (Sigma Aldrich, St. Louis, MO, U.S.A) was prepared as pre-mix and transferred to the IBIDI 8 well microscopy chamber. Confocal pictures were taken on a TCS SP8 confocal microscope (Leica Microsystems, Mannheim, Germany) equipped with an HCX PL APO 63x 1.2 N.A. water immersion lens immediately after 20 min of incubation with peptides. Carboxyfluorescein fluorescence was excited using the 488 nm line of a white laser (WLL) and fluorescence detected at 500 - 550 nm.

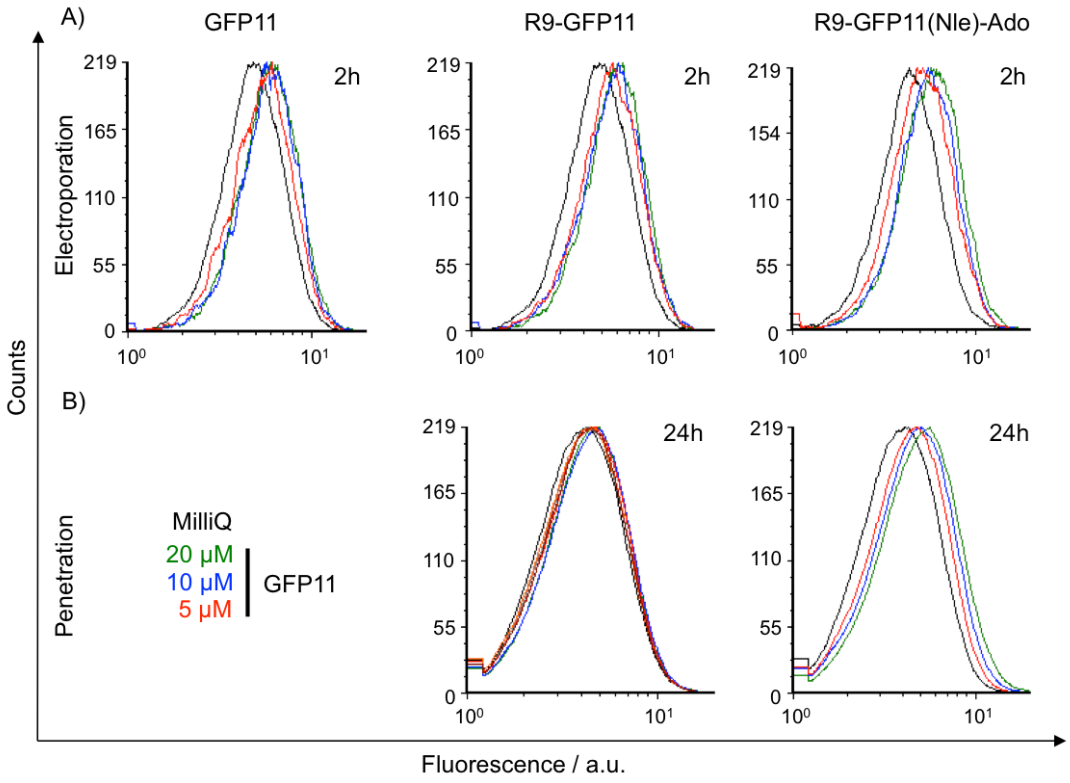

Supplemental Figure 1. Dose dependence of GFP complementation after A) long-term recovery and B) penetration. GFP11 peptides were introduced into HEK293T cells transfected with standard GFP1-10 either by electroporation or by penetration. Fluorescence of GFP was detected by flow cytometry from morphologically intact cells gated based on forward versus sideward scatter 2 h after electroporation or 24 h after CPP-mediated import.

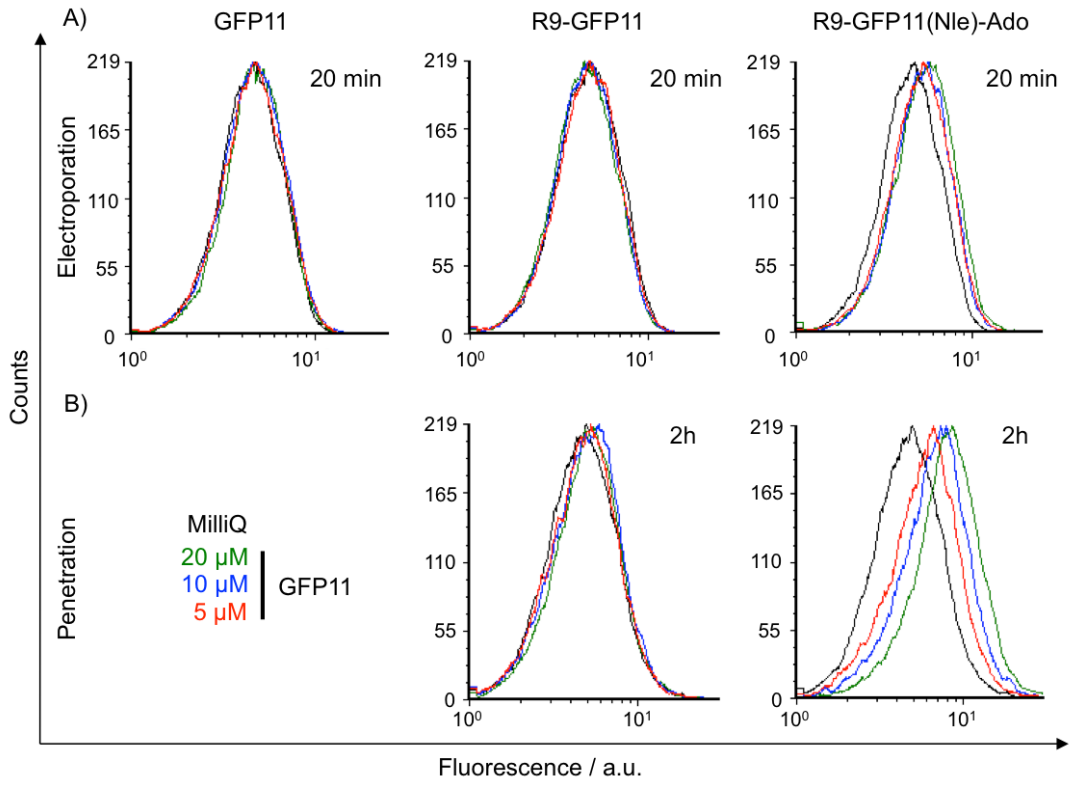

Supplemental Figure 2. Dose dependence of GFP complementation after A) short-term recovery and B) penetration. GFP11 peptides were introduced into HEK293T cells transfected with standard GFP1-10 either by electroporation or by CPP-mediated import. Fluorescence of GFP was detected by flow cytometry from morphologically intact cells gated based on forward versus sideward scatter 20 min after electroporation or 2 h after CPP-mediated import.

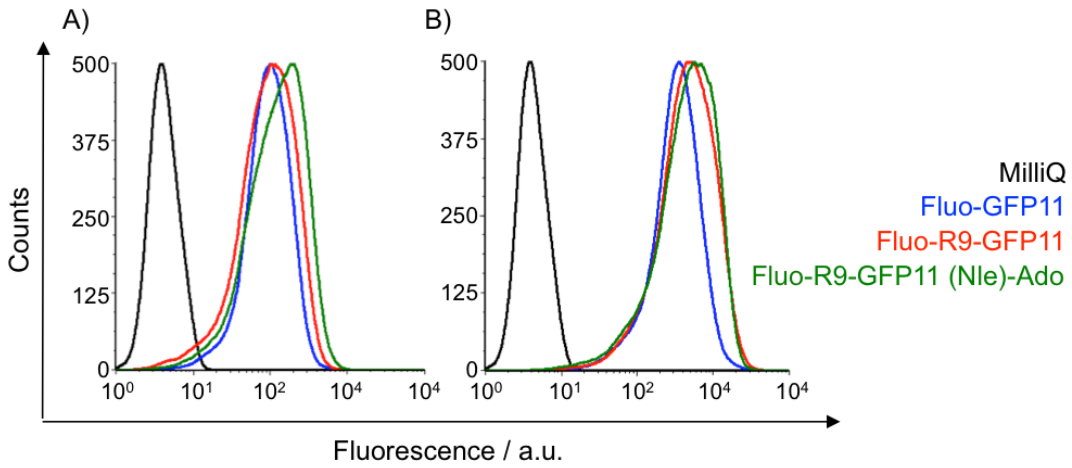

Supplemental Figure 3. Comparison of electroporation efficiencies. Peptides, as indicated by color were introduced into HEK293T cells by electroporation with either A) 2.5 µM or B) 10 µM final concentration in the cuvette. Cells were transferred into culture medium with 10% serum and without phenol red, returned to the incubator for recovering from the electroporation procedure for 20 min. Afterwards intracellular fluorescence was measured in the presence of 0.4 % trypan blue by flow cytometry. Trypan blue served to quench fluorescence from peptide associated to the outside of the cells, which may be the case in particular for the R9-elongated peptides. Fluorescence resulting from morphologically intact cells was gated based on forward versus sideward scatter.

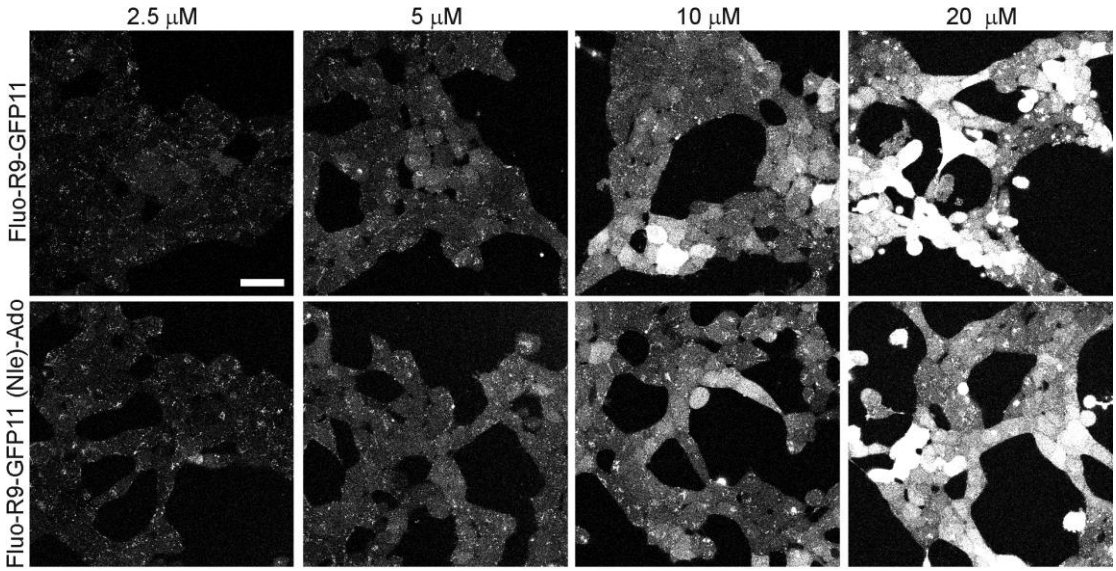

Supplemental Figure 4. Concentration dependence of import and intracellular peptide distribution for Carboxyfluorescein-labeled analogs. HEK293T cells were incubated with peptides at the indicated concentrations over 20 min in the absence of serum. The scale bar corresponds to 20 μm.

A)

Carboxyfluorescein-RRRRRRRRRGSTSRDHMVLHEYVNAAGIT-NH2

Carboxyfluorescein-RRRRRRRRRGSTSRDHNLeVLHEYVNAAGIT-Ado-NH2

B)

Ac-RRRRRRRRRGSTSRDHMVLHEYVNAAGIT-NH2

Ac-RRRRRRRRRGSTSRDHNLeVLHEYVNAAGIT-Ado-NH2

C)

MVSKGEEDNMAIIKEFMRFKVHMEGSVNGHEFEIEGEGEGRPYEGTQTAKLK
VTKGGPLPFAWDILSPQFMYGSKAYVKHPADIPDYLKLSFPEGFKWERVMNFE
DGGVVTVTQDSSLQDGEFIYKVKLRGTNFPSDGPVMQKKTMGWEASSERMY
PEDGALKGEIKQRLKLKDGGHYDAEVKTTYKAKKPVQLPGAYNVNIKLDITS
HNEDYTIVEQYERAEGRHSTGGMDELYKEGRGSLLTCGDVEENAAPGSMSKG
EELFTGVVPILVELDGDVNGHKFSVRGEGEGDATIGKLTLKFICTTGKLPVPWP
TLVTTLTYGVQCFSRYPDHMKRHDFFKSAMPEGYVQERTISFKDDGKYKTRAV
VKFEGDTLVNRIELKGTDFKEDGNILGHKLEYNFNSHNVYITADKQKNGIKAN
FTVRHNVEDGSVQLADHYQQNTPIGDGPVLLPDNHYLSTQTVLSKDPNEK*

Supplemental Figure 5. The peptide sequence of A) Carboxyfluorescein-labeled and B) acetylated R9-GFP11 variants and C) the amino acid sequence of the mCherry-GFP1-10 fusion protein. A) and B) Highlighted in blue: Linker, highlighted in red: non-natural amino acid norleucine, highlighted in green: C-terminal PEG-moiety Ado (8-amino-3,6-dioxaoctanoic acid). C) Highlighted in red: mCherry, highlighted in green: GFP1-10. The amino acids in between mCherry and GFP1-10 represent the linker. The STOP-codon is denoted by the asterisk at the end of the sequence.

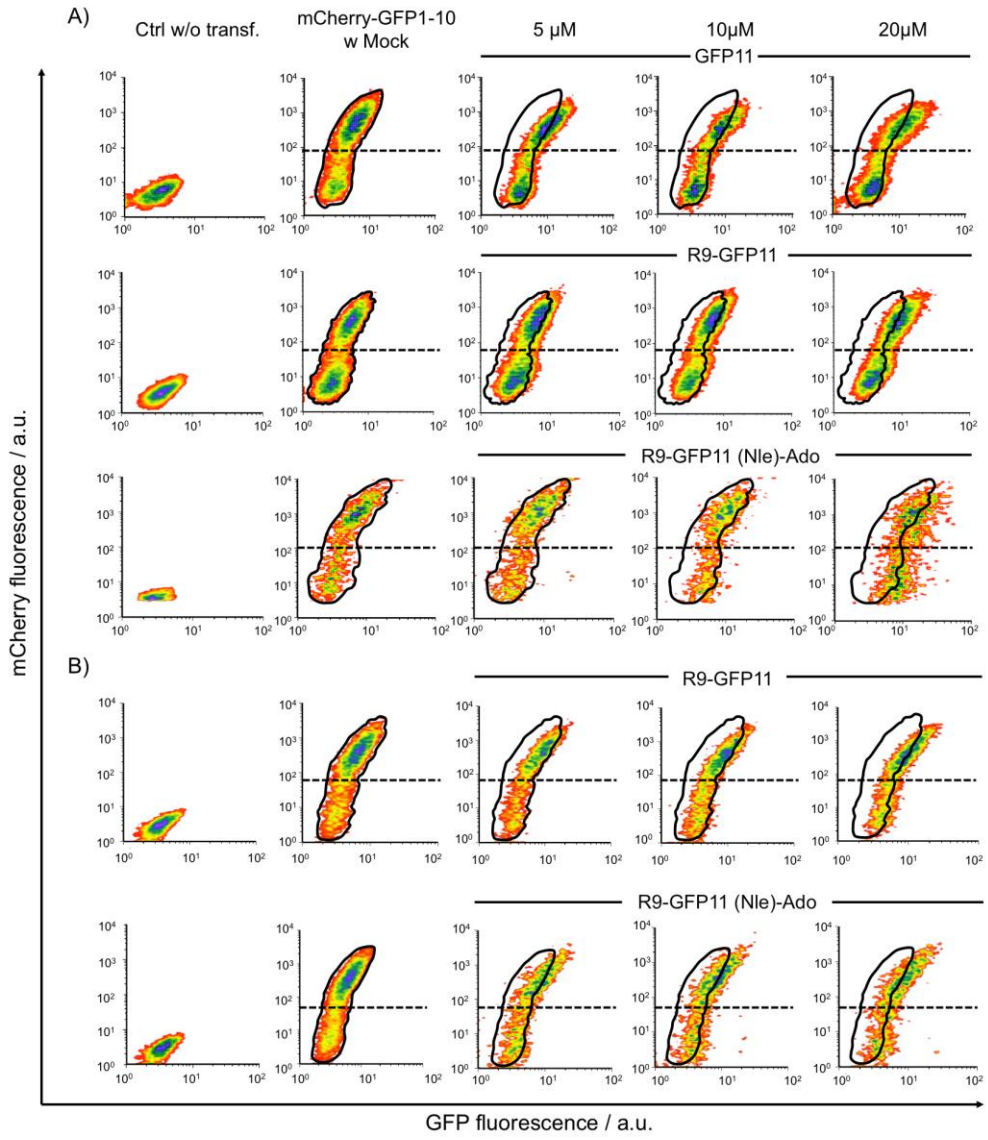

Supplemental Figure 6. Density plots showing the dose dependence of GFP complementation for high and low mCherry expressing cells (line gate) and for only high mCherry positive cells (population above the dashed line) after short-term treatment with GFP11 variants. HEK293T cells were transfected with mCherry-GFP1-10 followed by A) electroporation with the GFP11 variants and subsequent recovery for 20 min or B) by penetration at the indicated concentrations for 2 h at 37°C. Mock samples were incubated with MillQ instead of GFP11 variants. Fluorescence of GFP was detected by flow cytometry from morphologically intact cells gated based on forward versus sideward scatter. The density plots are representative for at least two independent experiments.

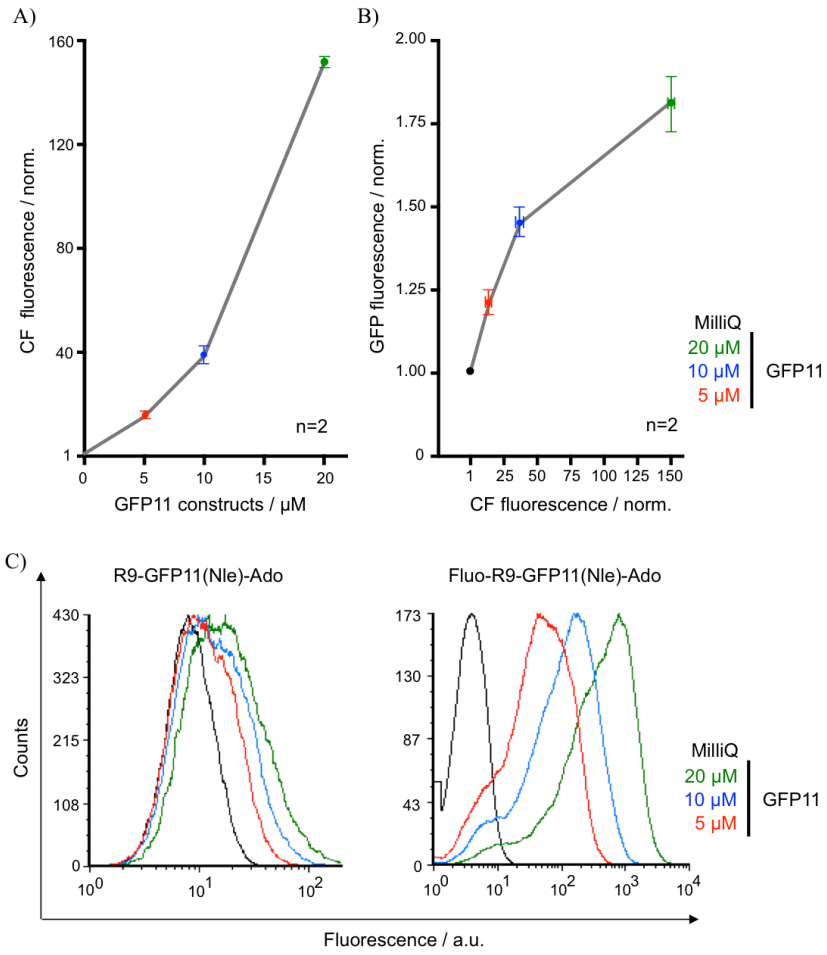

Supplemental Figure 7. The dose dependent GFP fluorescence intensity is directly related to the cytosolic concentration of the GFP-11 variants. A) - C) HEK293T cells were transfected with mCherry-GFP1-10 followed by electroporation of R9-GFP11 or carboxyfluorescein labeled R9-GFP11 analogs at the indicated concentrations. Fluorescence for both, GFP and carboxyfluorescein (CF) was detected by flow cytometry from morphologically intact cells gated based on forward versus sideward scatter after 20 min (R9-GFP11) or directly after electroporation (Carboxyfluorescein-R9-GFP11). The GFP fluorescence of the GFP11 variants was normalized to the background signal acquired from mock-treated cells incubated with MillQ instead of GFP11 variants. A) Dose response curve representing the concentration-dependent increase of the carboxyfluorescein signal in the cyosol. B) Correlation of the dose-dependent increase of GFP fluorescence and cell-associated carboxyfluorescein signal obtained from the respective pairs of samples. C) GFP and carboxyfluorescein fluorescence intensity histograms of one representative experiment. Error bars denote the standard error of the mean (SEM).

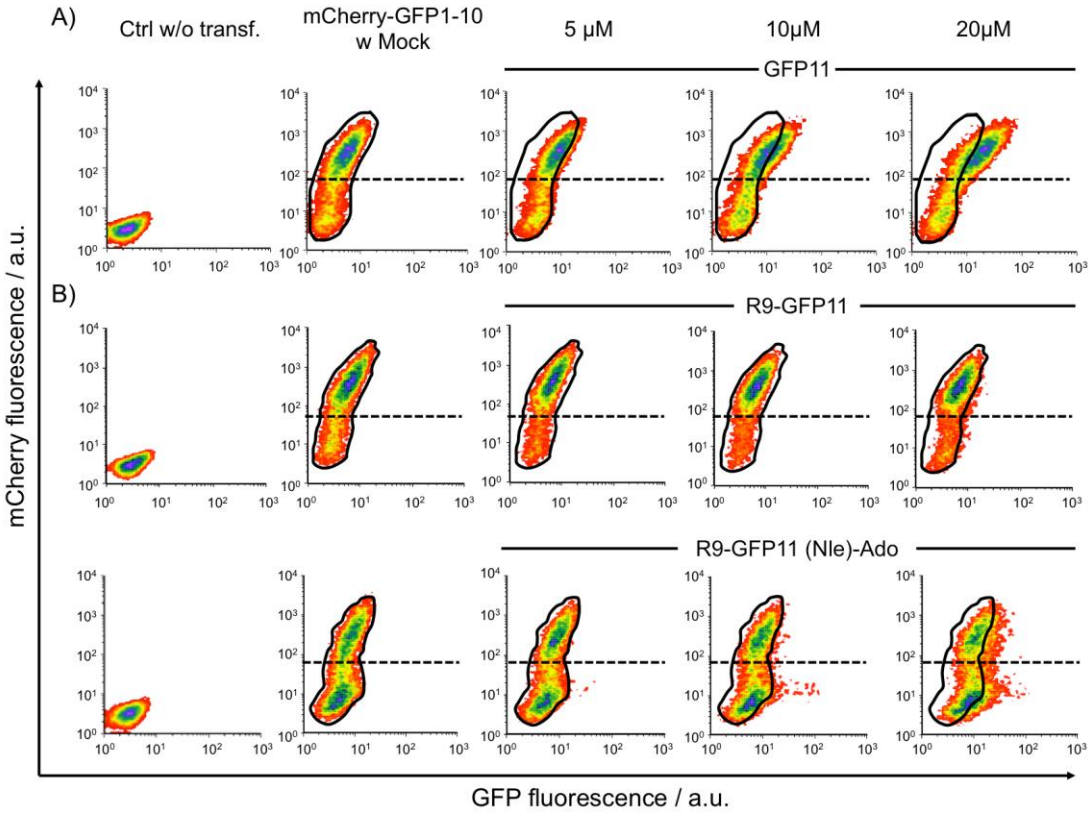

Supplemental Figure 8. Density plots showing the dose dependence of GFP complementation for high and low mCherry expressing cells (line gate) and for only high mCherry positive cells (population above the dashed line) after long-term treatment with GFP11 variants. HEK293T cells were transfected with mCherry-GFP1-10 followed by A) electroporation with the GFP11 variants and subsequent recovery for 2 h or B) by penetration at the indicated concentrations for 24 h at 37°C. Mock samples were incubated with MillQ instead of GFP11 variants. Fluorescence of GFP was detected by flow cytometry from morphologically intact cells gated based on forward versus sideward scatter. The density plots are representative for at least two independent experiments.

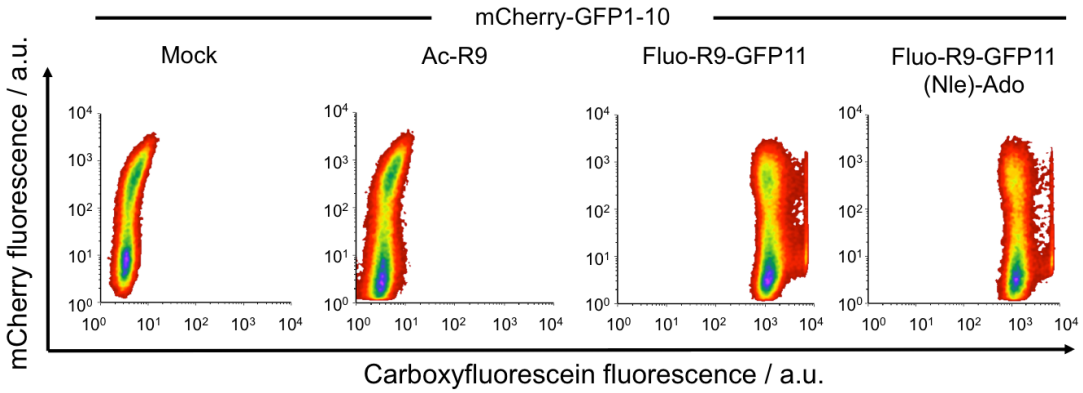

Supplemental Figure 9. Density plots for HEK293T cells, showing equivalent uptake efficiencies of carboxyfluorescein labeled R9-GFP11 analogs in cells expressing high and low levels of the mCherry-GFP1-10 fusion construct. Cells were transfected with mCherry-GFP1-10 followed by incubation with carboxyfluorescein-R9-GFP11 analogs, and acetylated R9 as a background control at 5 μM concentration or incubated with MillQ instead of GFP11 variants for 30 min at 37°C. Fluorescence for mCherry and fluorescein were detected by flow cytometry from morphologically intact cells gated based on forward versus sideward scatter. The density plots are representative for two independent experiments.

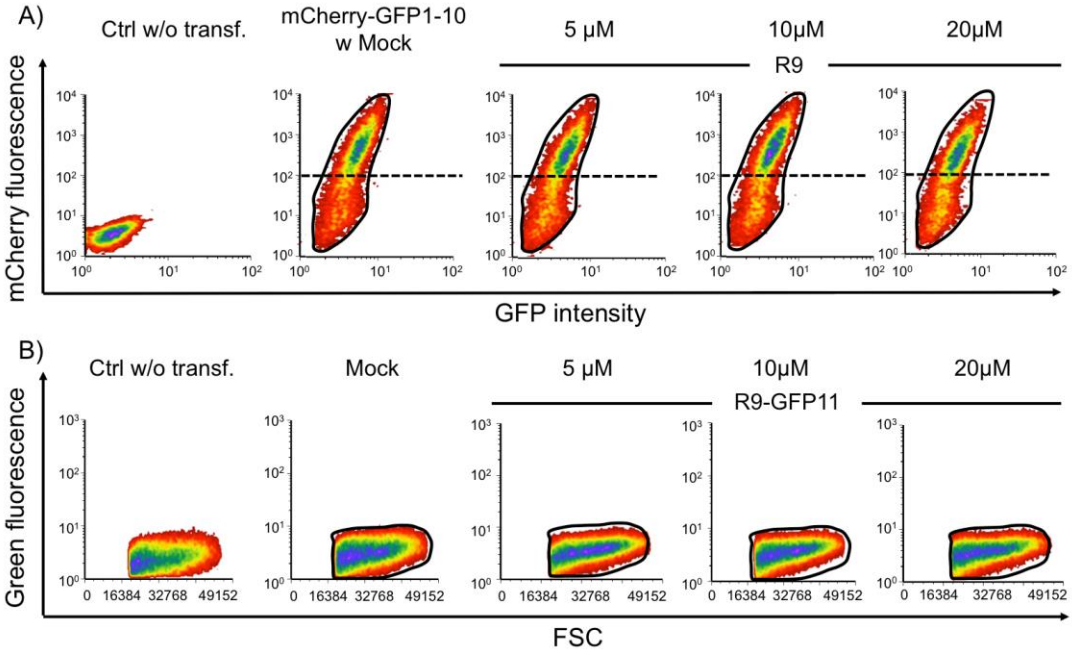

Supplemental Figure 10. Density plots for control samples. HEK293T cells were A) transfected with mCherry-GFP1-10 followed by incubation with R9 or B) Mock transfected followed by penetration with R9-GFP11 at the indicated concentrations for 24 h at 37°C. Mock samples were incubated with MillQ instead of GFP11 variants. Fluorescence for GFP was detected by flow cytometry from morphologically intact cells gated based on forward versus sideward scatter. The density plots are representative for at least two independent experiments.

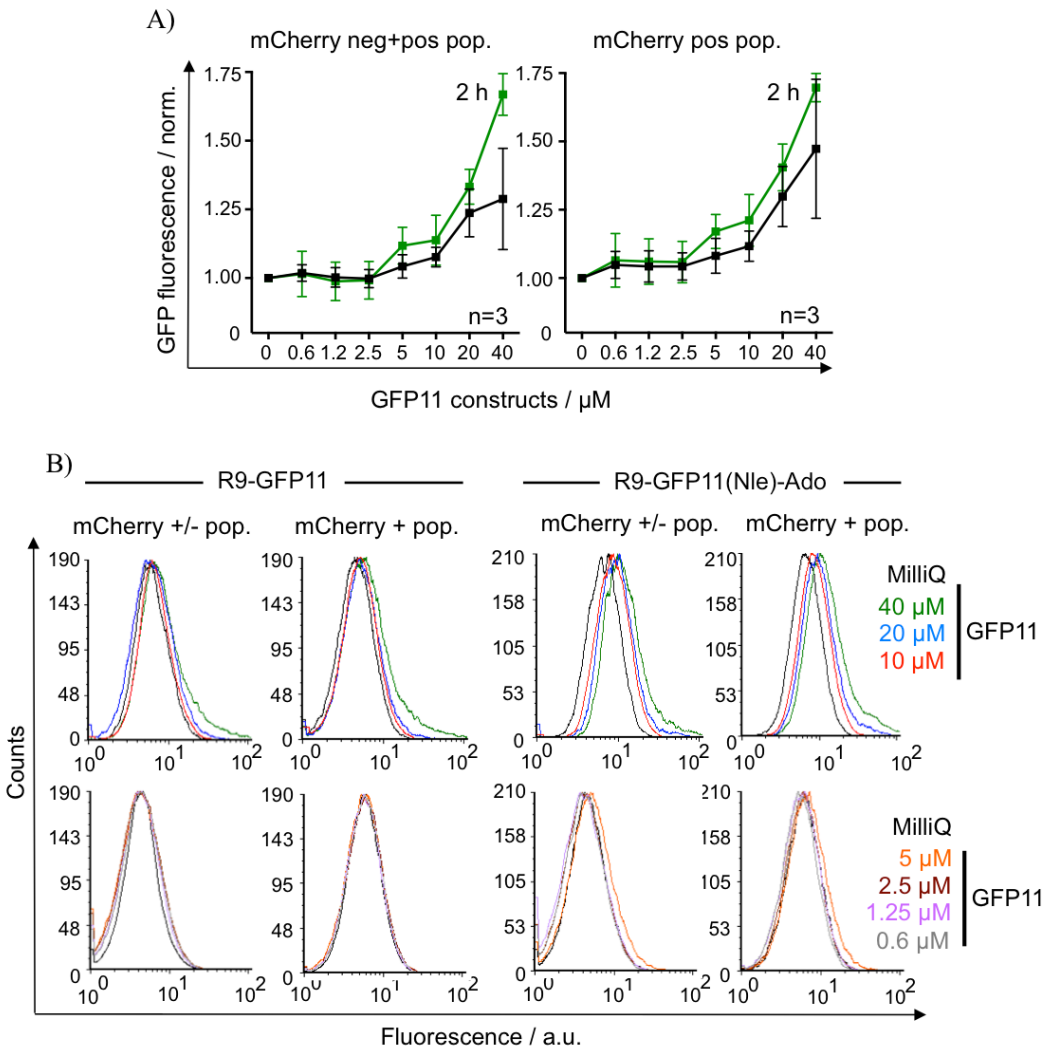

Supplemental Figure 11. Dose dependence of GFP complementation for the mCherry-GFP1-10 fusion protein over an extended concentration range. A, B) Fluorescence for both, mCherry and GFP was detected by flow cytometry from morphologically intact cells gated based on forward versus sideward scatter after 2 h incubation with peptides in FCS-free medium. The GFP fluorescence either for all cells (left) or for mCherry-positive cells was normalized to the background signal acquired from mock-treated cells. A) Curves indicate the average of the normalized medians of 3 independent experiments and B) GFP fluorescence intensity histograms of one representative experiment. Error bars denote the standard error of the mean (SEM). The data in (A) is a combination of two sets of experiments, one set testing concentrations from 0.6 to 5 µM and one set testing concentrations from 10 to 40 µM as indicated in (B). This was possible because of the normalization of the fluorescence increase.